Research Journal of Applied Sciences, Engineering and Technology 7(8): 1489-1499, 2014
DOI:10.19026/rjaset.7.424
ISSN: 2040-7459; e-ISSN: 2040-7467

Submitted: May 03, 2013 Accepted: June 01, 2013 Published: February 27, 2014

Research Article

Modeling and Simulation of Current Source Inverter Fed Synchronous Motor in Complex Frequency Domain Taking the Transition Zone From Induction Motor to Synchronous Motor Mode into Account

A.B. Chattopadhyay and Sunil Thomas
Department of Electrical and Electronics Engineering, Birla Institute of Technology and Science, Pilani-Dubai Campus, P.O. Box 345055, Plot No. UG 06, Dubai International Academic City, Dubai, U.A.E

Abstract: Modeling of synchronous motor plays a dominant role in designing complicated drive system for different applications, especially large blower fans etc for steel industries. As synchronous motor has no inherent starting torque generally it is started as an induction motor with the help of a damper winding and it pulls into synchronism under certain conditions. The present paper exactly concentrates on this particular zone of transition from induction motor to synchronous motor mode for a current source inverter fed synchronous motor drive system. Due to complexity of synchronous motor in terms of number of windings and finite amount of air gap saliency, direct modeling of such transition zone in time domain becomes cumbersome at the first instance of modeling. That is why the modeling in complex frequency domain (s-domain) has been taken up using small perturbation model. Such a model clearly shows role of induction motor as noise function or disturbance function with respect to the open loop block diagram of synchronous motor. Such finding can be quantized in terms of important results and that is done in the present paper such that the results can help the designer for the successful design of a synchronous motor drive system.

Keywords: Current source inverter, computer simulation, induction motor, small perturbation model, starting transients, synchronous machine

INTRODUCTION

Many constant speed applications such as fans, fuel pump and compressors comprising a considerable amount of total electrical appliances (Isfahani and Vaez-Zadeh, 2011) basically need a 3 phase synchronous motor. Even though permanent magnet synchronous motors are widely used in such applications, current source inverter fed normal synchronous motors can also be applied in many constant speed applications (Knight and McClay, 2000; Weifu *et al*., 2012). The steady state stability study of a current source inverter fed synchronous motor was basically initiated in 1974 (Gordon *et al*., 1974) and after this as an extension, (Chattopadhyay *et al*., 2011) presented a detailed analysis of a current source inverter fed synchronous motor drive system taking damper windings into account in 2011(Chattopadhyay *et al*., 2011). So far the research accuracy of the paper by (Chattopadhyay *et al*., 2011) is covered; it is not clear that exactly what is happening in the transition zone when the machine is jumping from induction motor action to synchronous motor action. Again the concentration on such detailed aspect is a matter of long discussion and in this context many researchers have tried to put sufficient light on the matter. The research paper (Xianhao *et al*., 2006) explains the analysis of magnetic fields and temperature fields for a salient pole synchronous motor in the process of steady state. They have used the d-q model of the synchronous motor but the role of field winding in transition from induction motor to synchronous motor is not reflected in the mathematical model.

A similar observation is valid on the other work Wang and Ren (2003), and it represents a good state variable model and its mathematic simulations in time domain. The research paper (Sergelen, 2007; Najafi and Kar, 2007) carries important works on the mathematical modeling of a salient pole synchronous motor supplied by a frequency converter and also the effect of short circuit voltage profile on the transient performance of permanent magnet synchronous motors .An important work on non-linear control of an inverter motor drive system with input filter (Marx *et al*., 2008) draws attention. In this paper the author has given a detailed signal analysis of the DC-link voltage stability.

Another interesting paper by Das and Casey (1999) and Al-Ohaly *et al*. (1997) clearly portrays the critical

Corresponding Author: Sunil Thomas, Department of Electrical and Electronics Engineering, Birla Institute of Technology and Science, Pilani-Dubai Campus, Dubai International Academic City, Dubai, U.A.E, P.O. Box 345055, Plot No. UG 06, Tel.: (009714) 4200700 extn. 225 Fax: (009714) 4200555

aspects of starting a large synchronous motor. Even though this particular work does not involve much mathematical analysis but the range of the slip presented in this paper with reference to pull in torque of a synchronous motor really may help a designer to select a particular synchronous motor for any specific application.

Based on the above said literature review, to the best of the authors understanding it reveals that researchers have not put sufficient light on the fact that exactly what happens to the mathematical model of a synchronous motor in time domain or complex frequency domain during the period when field winding is disconnected from the external resistance (generally 6-7 times of main field winding resistance to avoid effects due to George's phenomenon) and immediately thrown to the DC source. In the authors opinion investigation in such direction becomes very much crucial because before connecting the field winding to the DC source characterization of the machine can be done as 3 phase induction motor. Therefore, it will be very logical to get the semi induction semi synchronous machine character to be reflected in the resultant mathematical model. This particular work has been presented by the authors in the present paper. The strategy of formulation at this stage may not be necessary to feel the importance of the problem. But in the next section the mathematical methods will be explained in detail.

MATERIALS AND METHODS

The basic block diagram of the proposed scheme is shown in Fig. 1.

To have a better feeling of the method of analysis, the primitive mac0068ine model of the synchronous motor is drawn and it is shown in Fig. 2.

In the following analysis, saturation is ignored but provision is made for inclusion of saliency and one number of damper winding on each axis. Following Park's transform, a constant stator current of value is at a field angle 'β' can be represented by direct and quadrature axis currents as:

$$i_d = i_s \cos\beta \tag{1}$$

$$i_q = i_s \sin b\beta \tag{2}$$

Designating steady state value by the subscript '0' and small perturbation byΔ, the perturbation equations of the machines are:

$$\Delta i_d = -i_s \sin\beta_0 \Delta\beta \tag{3}$$

$$\Delta i_q = i_s \cos\beta_0 \Delta\beta \tag{4}$$

The transformed version of Eq. (3) and (4) are:

$$\Delta I_d(s) = -i_s \sin\beta_0 \Delta\beta(s) \tag{5}$$

$$\Delta I_q(s) = i_s \cos\beta_0 \Delta\beta(s) \tag{6}$$

The generalized expression for electromagnetic torque of a primitive machine model is an established one and it is expressed as:

$$\begin{aligned} T_e &= \Psi_d i_q - i_d \Psi_q \\ &= \left(L_d i_d + L_{md} i_f + L_{md} i_{kd}\right) i_q - \left(L_q i_q + L_{mq} i_{kq}\right) i_d \\ &= \left(L_d - L_q\right) i_d i_q + L_{md} i_q i_f + L_{md} i_{kd} i_q - L_{mq} i_{kq} i_d \end{aligned} \tag{7}$$

Small signal version of torque equation in time domain is expressed as:

$$\begin{aligned} \Delta T_e = {} & \left(L_d - L_q\right)\Delta i_d i_{q0} + \left(L_d - L_q\right)\Delta i_q i_{d0} + L_{md}\Delta i_q i_{f0} + L_{md}\Delta i_f i_{q0} \\ & + L_{md}\Delta i_{kd} i_{q0} + L_{md} i_{kd0}\Delta i_q - L_{mq}\Delta i_{kq} i_{d0} - L_{mq} i_{kq0}\Delta i_d \end{aligned} \tag{8}$$

Equation (8) after being transformed takes the shape as given by:

$$\begin{aligned} \Delta T_e(s) = {} & \left(L_d - L_q\right) i_{q0}\Delta I_d(s) + \left(L_d - L_q\right) i_{d0}\Delta I_q(s) + L_{md} i_{f0}\Delta I_q(s) + L_{md} i_{q0}\Delta I_f(s) \\ & + L_{md} i_{q0}\Delta I_{kd}(s) + L_{md} i_{kd0}\Delta I_q(s) - L_{mq} i_{d0}\Delta I_{kq}(s) - L_{mq} i_{kq0}\Delta I_d(s) \\ = {} & \left[\left(L_d - L_q\right) i_{q0} - L_{mq} i_{kq0}\right]\Delta I_d(s) + \left[\left(L_d - L_q\right) i_{d0} + L_{md} i_{kd0} + L_{md} i_{f0}\right]\Delta I_q(s) \\ & + L_{md} i_{q0}\Delta I_f(s) + L_{md} i_{q0}\Delta I_{kd}(s) - L_{mq} i_{d0}\Delta I_{kq}(s) \end{aligned} \tag{9}$$

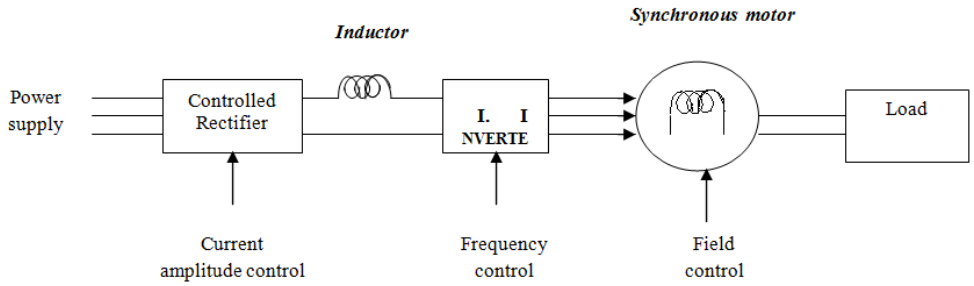

Fig. 1: Drive configuration for open-loop current-fed synchronous motor control

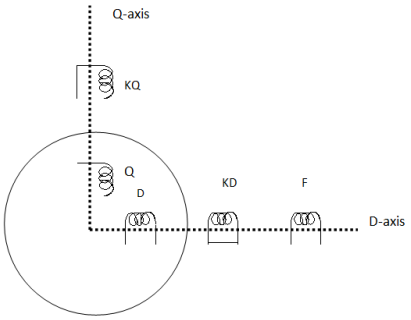

Fig. 2: Primitive machine model of a synchronous motor

To tackle Eq. (9) in an easier form, it is expressed as:

$$\Delta T_e(s) = c_1\Delta I_d(s) + c_2\Delta I_q(s) + c_3\Delta I_f(s) + c_4\Delta I_{kd}(s) + c_5\Delta I_{kq}(s) \quad (10)$$

where,

$$c_1 = \left[\left(L_d - L_q\right)i_{q0} - L_{mq}i_{kq0}\right] \quad (11a)$$

$$c_2 = \left[\left(L_d - L_q\right)i_{d0} + L_{md}i_{kd0} + L_{md}i_{f0}\right] \quad (11b)$$

$$c_3 = L_{md}i_{q0} \quad (11c)$$

$$c_4 = L_{md}i_{q0} \quad (11d)$$

$$c_5 = -L_{mq}i_{d0} \quad (11e)$$

The small perturbation model of the transformed voltage balance equations of F-coil, KD-coil and KQ are expressed as:

$$\frac{c}{s} + s_1\frac{k}{s} = \Delta U_f(s) = R_f\Delta I_f(s) + sL_{ff}\Delta I_f(s) + sL_{md}\Delta I_d(s) + sL_{md}\Delta I_{kd}(s) \quad (12)$$

where,
c = 220 Volts
S_1 = Slip
k = $(N_f/Na)*(415/\sqrt{3})$
N_f = Number of turns in field winding
Na = Number of turns in armature winding:

$$0 = \Delta U_{kd}(s) = R_{kd}\Delta I_{kd}(s) + sL_{kkd}\Delta I_{kd}(s) + sL_{md}\Delta I_d(s) + sL_{md}\Delta I_f(s) \quad (13)$$

$$\Delta U_{kq}(s) = R_{kq}\Delta I_{kq}(s) + sL_{kkq}\Delta I_{kq}(s) + sL_{mq}\Delta I_q(s) \quad (14)$$

where,
c = 220 Volts
S_1 = Slip
k = $(N_f/Na)*(415/\sqrt{3})$
N_f = Number of turns in field winding
Na = Number of turns in armature winding

As the damper winding on d-axis and q-axis are short-circuited within themselves, $\Delta U_{kd} = 0$ and $\Delta U_{kq} = 0$. So in transformed version $\Delta U_{kd}(s) = 0$ and $\Delta U_{kq}(s) = 0$ as shown in Eq. (13) and (14). Furthermore in general, the voltage fed to the field winding is fixed. It is a well known fact that a synchronous motor cannot start for itself and the easiest way to start a synchronous motor is to start it as an induction machine with the help of damper windings. But the problem is that we have to investigate what will be status of field winding of the synchronous motor when the damper winding is in action. As already the winding was physically embedded (existing), and during the running of the machine one cannot take it out. In other words when damper winding is in action field winding effect has to be inactivated. Such inactivation may be done by the following methods:

(a) Field winding completely Open Circuit
(b) Field Winding Short Circuit in itself

The status of field winding in (a) can be looked upon as a transformer whose primary winding constitutes of 3 phase armature winding supplied from 415 V (L-L) ac and whose secondary winding is the field winding being open circuited. As generally in a normal synchronous machine of normal design $N_f/N_a >> 1$, where N_f is number of field windings and N_a is number of armature windings. The induced voltage in the open field terminal will be large and it may lead to hazardous conduction so far as operator safety is concerned. Hence this case is rejected.

Status of the field winding in (b): The induced emf in field winding due to transformer action will produce a single phase alternating current and in turn will produce a pulsating field in field winding. It is well known that a pulsating field m.m.f can be resolved as a combination of forward rotating and backward rotating m.m.f magnetic fields (strengths of each resolved component is half of the original pulsating m.m.f). The effect of backward rotating magnetic field will produce a torque opposite to the (asynchronous/induction) motor torque and it will dominate at some value of slip. Hence a situation may arise and motor may stall due to the negative effect of backward component. This phenomenon is known as George's phenomenon.

Hence such case cannot be completely accepted. However there is some remedial method. The field winding may be closed through an external resistance which is about 6-7 times of original field resistance; such that the magnitude of short circuit current diminishes and as a result effect of resolved backward component will be less or reduced.

What happens to change on field voltage (ΔU_f): In the current research problem ΔU_f cannot be equal to zero because originally it was an induction motor with

the field winding short circuited in it or closed through an external resistance of large value and at a later stage it was pulled into synchronism when dc supply is fed to the winding.

Quantitatively, ΔU_f should depend on a particular property of induction motor and that property must be 'SLIP'. Here the technique of mathematical modeling appears as a novel approach and this approach forms the foundation of the proposed analysis. The proposed modeling considers that field winding is closed within itself. In other words the presence of external large resistance has not been considered in modeling to make the mathematical treatment comparatively easy. However it does not affect the accuracy of the system as the external resistance can be lumped or clubbed with the field winding.

From Eq. (12) and (13) it yields:

$$\Delta I_f(s)=\left(\frac{s^2(L_{md}{}^2-L_{md}L_{kkd})-sL_{md}R_{kd}}{s^2(L_{kkd}L_{ff}-L_{md}{}^2)+s(L_{kkd}R_f+R_{kd}L_{ff})+R_{kd}R_f}\right)\Delta I_d(s)-\mathrm{F}_{32}(\mathrm{s}) \quad (15)$$

where,

$$\mathrm{F}_{32}(\mathrm{s})=(R_{kd}+sL_{kkd})[\frac{c+s_1k}{s^2L_{md}}] \quad (16)$$

Similarly Eq. (12) and (13) yields:

$$\Delta I_{kd}(s)=F_{31}(s)-\left(\frac{s^2(L_{md}{}^2-L_{md}L_{ff})-sL_{md}R_f}{s^2(L_{kkd}L_{ff}-L_{md}{}^2)+s(L_{kkd}R_f+R_{kd}L_{ff})+R_{kd}R_f}\right)\Delta I_d(s)$$

$$= F_{31}(s)-\left(\frac{d_1s^2+d_2s}{D(s)}\right)\Delta I_d(s) \quad (17)$$

where,

$$F_{31}(s)=\frac{\mathrm{c}+\mathrm{s}_1\mathrm{k}}{s^2}\left[1-\left\{\left(\frac{R_f}{SL_{md}}+\frac{L_{ff}}{L_{md}}\right)\left(R_{kd}+sL_{kkd}\right)\right\}\right] \quad (18)$$

$$\mathrm{d}_1=\left(\mathrm{L}_{\mathrm{md}}{}^2-\mathrm{L}_{\mathrm{md}}\mathrm{L}_{\mathrm{ff}}\right) \quad (18a)$$

$$\mathrm{d}_2=-\mathrm{L}_{\mathrm{md}}\mathrm{R}_{\mathrm{f}} \quad (18b)$$

From Eq. (14) it is obtained:

$$\Delta I_{kq}(s)=\left(\frac{-sL_{mq}}{R_{kq}+sL_{kkq}}\right)\Delta I_q(s) \quad (19)$$

$$=\left(\frac{e_1s}{Q(s)}\right)\Delta I_q(s) \quad (20)$$

where,

$$\mathrm{e}_1=-\mathrm{L}_{\mathrm{mq}} \quad (20a)$$

$$\mathrm{Q(s)}=\mathrm{f}_1\mathrm{s}+\mathrm{f}_2 \quad (20b)$$

$$\mathrm{f}_1=\mathrm{L}_{\mathrm{kkq}} \quad (20c)$$

$$\mathrm{f}_2=\mathrm{R}_{\mathrm{kq}} \quad (20d)$$

Substituting Eq. (15), (17), (19) in Eq. (10), it yields:

$$\Delta T_e(s)=c_1\Delta I_d(s)+c_2\Delta I_q(s)+c_3\left[\frac{a_1s^2+a_2s}{D(s)}\right]\Delta I_d(s)+c_4\left[\frac{d_1s^2+d_2s}{D(s)}\right]\Delta I_d(s)+c_5\left[\frac{e_1s}{Q(s)}\right]\Delta I_q(s)$$
$$=\left[c_1+\frac{c_3a_1s^2+c_3a_2s+c_4d_1s^2+c_4d_2s}{D(s)}\right]\Delta I_d(s)+\left[c_2+\frac{c_5e_1s}{Q(s)}\right]\Delta I_q(s)+\mathrm{F}_3(\mathrm{s}) \quad (21)$$

where,

$$\mathrm{F}_3(\mathrm{s})=\mathrm{F}_{31}(\mathrm{s})-\mathrm{F}_{32}(\mathrm{s}) \quad (22)$$

Equation (21) can be re expressed as:

$$\Delta T_e(s)=\left[\frac{(m_1s^3+m_2s^2+m_3s+m_4)\Delta I_d(s)+(n_1s^3+n_2s^2+n_3s+n_4)\Delta I_q(s)}{l_1s^3+l_2s^2+l_3s+l_4}\right]+\mathrm{F}_3(\mathrm{s}) \quad (23)$$

where,

$$\mathrm{m}_1=\mathrm{f}_1\mathrm{c}_1\mathrm{b}_1+\mathrm{c}_3\mathrm{a}_1\mathrm{f}_1+\mathrm{c}_4\mathrm{d}_1\mathrm{f}_1 \quad (23a)$$

$$\mathrm{m}_2=\mathrm{c}_1\mathrm{f}_1\mathrm{b}_2+\mathrm{c}_3\mathrm{a}_2\mathrm{f}_1+\mathrm{c}_4\mathrm{d}_2\mathrm{f}_1+\mathrm{c}_1\mathrm{b}_1\mathrm{f}_2+\mathrm{c}_3\mathrm{a}_1\mathrm{f}_2+\mathrm{c}_4\mathrm{d}_1\mathrm{f}_2 \quad (23b)$$

$$\mathrm{m}_3=\mathrm{c}_1\mathrm{b}_2\mathrm{f}_2+\mathrm{c}_3\mathrm{a}_2\mathrm{f}_2+\mathrm{c}_4\mathrm{d}_2\mathrm{f}_2+\mathrm{c}_1\mathrm{b}_3\mathrm{f}_1 \quad (23c)$$

$$\mathrm{m}_4=\mathrm{c}_1\mathrm{b}_3\mathrm{f}_2 \quad (23d)$$

$$\mathrm{n}_1=\mathrm{f}_1\mathrm{c}_2\mathrm{b}_1+\mathrm{c}_5\mathrm{e}_1\mathrm{b}_1 \quad (23e)$$

$$\mathrm{n}_2=\mathrm{c}_2\mathrm{f}_2\mathrm{b}_1+\mathrm{c}_2\mathrm{f}_1\mathrm{b}_2+\ \mathrm{c}_5\mathrm{e}_1\mathrm{b}_2 \quad (23f)$$

$$\mathrm{n}_3=\mathrm{c}_2\mathrm{f}_2\mathrm{b}_2+\mathrm{b}_3\mathrm{c}_2\mathrm{f}_1+\mathrm{b}_3\mathrm{c}_5\mathrm{e}_1 \quad (23g)$$

$$\mathrm{n}_4=\mathrm{c}_2\mathrm{f}_2\mathrm{b}_3 \quad (23h)$$

$$\mathrm{l}_1=\mathrm{b}_1\mathrm{f}_1 \quad (23i)$$

$$\mathrm{l}_2=\mathrm{b}_2\mathrm{f}_1+\mathrm{b}_1\mathrm{f}_2 \quad (23j)$$

$$\mathrm{l}_3=\mathrm{b}_3\mathrm{f}_1+\mathrm{b}_2\mathrm{f}_2 \quad (23k)$$

$$\mathrm{l}_4=\mathrm{b}_3\mathrm{f}_2 \quad (23l)$$

Substituting the expressions for $\Delta I_d(s)$ and $\Delta I_q(s)$ from Eq. (3) and (4) in Eq. (23), we have:

$$\Delta T_e(s)=\left[\frac{(m_1s^3+m_2s^2+m_3s+m_4)(-i_s\sin\beta_0(s))+(n_1s^3+n_2s^2+n_3s+n_4)(i_s\cos\beta_0(s))}{l_1s^3+l_2s^2+l_3s+l_4}\right]\Delta\beta(s) + F_3(s) \quad (24)$$

Equation (24) can be re-expressed as:

$$\Delta T_e(s)=\left[\frac{x_1s^3+x_2s^2+x_3s+x_4}{l_1s^3+l_2s^2+l_3s+l_4}\right]\Delta\beta(s)+F_3(s) \quad (25)$$

$$\Delta T_e(s)=T_1(s)\Delta\beta(s)+F_3(s) \quad (25a)$$

where,

$$T_1(s)=\left[\frac{x_1s^3+x_2s^2+x_3s+x_4}{l_1s^3+l_2s^2+l_3s+l_4}\right] \quad (26)$$

$$x_1=n_1i_s\cos b_0-m_1i_s\sin b_0 \quad (26a)$$

$$x_2=n_2i_s\cos b_0-m_2i_s\sin b_0 \quad (26b)$$

$$x_3=n_3i_s\cos b_0-m_3i_s\sin b_0 \quad (26c)$$

$$x_4=n_4i_s\cos b_0-m_4i_s\sin b_0 \quad (26d)$$

The torque dynamic equation of a synchronous motor can be written as:

$$T_e-T_L=J\frac{d\omega}{dt} \quad (27)$$

where,

ω = Motor speed in mechanical rad./sec.

J = Polar moment of inertia of motor and load (combined)

The small change in speed 'ω' equal to $\Delta\omega$ can be related to small change in field angle, $\Delta\beta$ as given by:

$$\Delta\omega=-\frac{d(\Delta\beta)}{dt} \quad (28)$$

The negative sign in equation physically indicates a drop in speed (ω) due to increase in field angle (β).

Based on Eq. (28), the following expression can be written:

$$J\frac{d(\Delta\omega)}{dt}=J\frac{d}{dt}\left[-\frac{d}{dt}(\Delta\beta)\right]=-J\frac{d^2}{dt^2}(\Delta\beta) \quad (29)$$

The small-perturbation model of Eq. (27) can be written as:

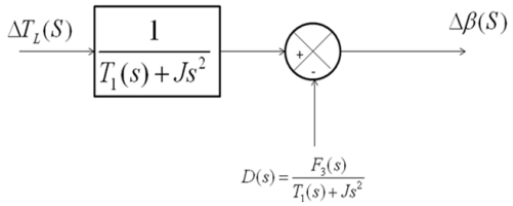

Fig. 3: Block diagram representation of the system with disturbance function D(s)

$$\Delta T_e-\Delta T_L=J\frac{d(\Delta\omega)}{dt} \quad (30)$$

Combining Eq. (29) and (30), it yields:

$$\Delta T_e-\Delta T_L=-J\frac{d^2}{dt^2}(\Delta\beta) \quad (31)$$

The transformed version of Eq. (31), with initial condition relaxed, comes out to be:

$$T_e(s)-T_L(s)=-Js^2\Delta\beta(s) \quad (32)$$

Substituting the expression for $\Delta Te(s)$ from Eq. (25) in (32), we have:

$$T_1(s)\Delta\beta(s)+Js^2\Delta\beta(s)+F_3(s)=\Delta T_L(s) \quad (33)$$

$$\frac{1}{\left[T_1(s)+Js^2\right]}\Delta T_L(s)-\frac{1}{\left[T_1(s)+Js^2\right]}F_3(s)=\Delta\beta(s) \quad (34)$$

The block diagram representation of the system obtained from the above equation is shown in Fig. 3.

The disturbance function can be taken separately and a detailed analysis in complex frequency domain is carried out as follows:

$$F_3(s)=F_{31}(s)-F_{32}(s) \quad (35)$$

where,

$$F_{32}(s)=(R_{kd}+sL_{kd})\left(\frac{c+s_1k}{s^2L_{md}}\right) \quad (36)$$

and:

$$F_{31}(s)=\frac{(c+s_1k)}{s^2}\left[1-\left(\frac{R_f}{sL_{md}}+\frac{L_{ff}}{L_{md}}\right)(R_{kd}+sL_{kd})\right] \quad (37)$$

$$F_{31}(s)=\frac{(c+s_1k)}{s^2}\left[1-\left(\frac{R_f}{sL_{md}}+\frac{L_{ff}}{L_{md}}\right)(R_{kd}+sL_{kd})\right] \quad (38)$$

Let $k_1=c+s_1k$

$$F_{31}(\mathrm{s}) = \frac{k_1}{s^2}\left[\frac{\left\{sL_{md} - R_f R_{kd} - s(\mathrm{L}_{kkd}\mathrm{R}_f + \mathrm{R}_{kd}\mathrm{L}_{ff}) - \mathrm{s}^2 L_{ff} L_{kkd}\right\}}{sL_{md}}\right] \quad (39)$$

$$F_{31}(\mathrm{s}) = \frac{k_1}{s^3 L_{md}}\left\{-\mathrm{s}^2 L_{ff} L_{kkd} + s(L_{md} - \mathrm{L}_{kkd}\mathrm{R}_f - \mathrm{R}_{kd}\mathrm{L}_{ff}) - R_f R_{kd}\right\} \quad (40)$$

$$F_{31}(\mathrm{s}) = \left(-\frac{k_1 L_{ff} L_{kkd}}{L_{md}}\right)\left(\frac{1}{s}\right) + \frac{k_1\left\{L_{md} - \mathrm{L}_{kkd}\mathrm{R}_f - \mathrm{R}_{kd}\mathrm{L}_{ff}\right\}}{s^2 L_{md}} - \left(\frac{R_f R_{kd} k_1}{L_{md}}\right)\frac{1}{s^3} \quad (41)$$

Let:

$$c_1 = \left(\frac{k_1 L_{ff} L_{kkd}}{L_{md}}\right) \quad (42)$$

$$c_2 = \frac{k_1\left\{L_{md} - \mathrm{L}_{kkd}\mathrm{R}_f - \mathrm{R}_{kd}\mathrm{L}_{ff}\right\}}{L_{md}} \quad (43)$$

$$c_3 = \left(\frac{R_f R_{kd} k_1}{L_{md}}\right) \quad (44)$$

Hence:

$$F_{31}(\mathrm{s}) = -c_1\left(\frac{1}{s}\right) + c_2\left(\frac{1}{s^2}\right) - c_3\left(\frac{1}{s^3}\right) \quad (45)$$

Put s = jω

$$F_{31}(\mathrm{j}\omega) = -c_1\left(\frac{1}{j\omega}\right) + c_2\left(\frac{1}{-\omega^2}\right) - c_3\left(\frac{1}{-j\omega^3}\right) \quad (46)$$

Since $\frac{1}{-j} = j$

$$\begin{aligned} F_{31}(\mathrm{j}\omega) &= jc_1\left(\frac{1}{\omega}\right) - c_2\left(\frac{1}{\omega^2}\right) - jc_3\left(\frac{1}{\omega^3}\right) \\ &= \left\{-\frac{c_2}{\omega^2}\right\} + j\left\{\frac{c_1}{\omega} - \frac{c_3}{\omega^3}\right\} \\ &= A_{31} + jB_{31} \end{aligned} \quad (47)$$

where,

$$A_{31} = -\frac{c_2}{\omega^2} \text{ and } B_{31} = \frac{c_1}{\omega} - \frac{c_3}{\omega^3} \quad (48)$$

$$\begin{aligned} F_{32}(\mathrm{s}) &= \left(R_{kd} + sL_{kkd}\right)\left(\frac{k_1}{s^2 L_{md}}\right) \\ &= \left(\frac{k_1}{L_{md}} R_{kd}\right)\frac{1}{s^2} + \left(\frac{k_1 L_{kkd}}{L_{md}}\right)\frac{1}{s} \end{aligned} \quad (49)$$

Let, $c_4 = \frac{k_1 R_{kd}}{L_{md}}$ and $c_5 = \frac{k_1 L_{kkd}}{L_{md}}$ (50)

$$F_{32}(\mathrm{s}) = \frac{c_4}{s^2} + \frac{c_5}{s} \quad (51)$$

Put s = jω

$$F_{32}(\mathrm{j}\omega) = -\frac{c_4}{\omega^2} - j\frac{c_5}{\omega} \quad (52)$$

$$= A_{32} + jB_{32} \quad (53)$$

where,

$$A_{32} = -\frac{c_4}{\omega^2} \,\&\, \mathrm{B}_{32} = \frac{c_5}{\omega} \quad (54)$$

$$\begin{aligned} F_3(\mathrm{j}\omega) &= \mathrm{F}_{31}(\mathrm{j}\omega) - \mathrm{F}_{32}(\mathrm{j}\omega) \\ F_3(\mathrm{j}\omega) &= A_3 + jB_3 \end{aligned} \quad (55)$$

$$\begin{aligned} A_3 &= A_{31} - A_{32} \\ &= -\frac{c_2}{\omega^2} + \frac{c_4}{\omega^2} = \frac{c_4 - c_2}{\omega^2} \\ B_3 &= \frac{c_1}{\omega} - \frac{c_3}{\omega^3} + \frac{c_5}{\omega} = \frac{c_1 + c_5}{\omega} - \frac{c_3}{\omega^3} \end{aligned} \quad (56)$$

$$\begin{aligned} &T_1(\mathrm{s}) + \mathrm{Js}^2 \\ &= \left\{\frac{X_1 s^3 + X_2 s^2 + X_3 s + X_4}{l_1 s^3 + l_2 s^2 + l_3 s + l_4}\right\} + Js^2 \end{aligned} \quad (57)$$

Put s = jω

$$\begin{aligned} &T_1(\mathrm{s}) + \mathrm{Js}^2\,|_{s=j\omega} \\ &= \left\{\frac{-jX_1\omega^3 - X_2\omega^2 + jX_3\omega + X_4}{-jl_1\omega^3 - l_2\omega^2 + jl_3\omega + l_4}\right\} - J\omega^2 \\ &= \left\{\frac{-jX_1\omega^3 - X_2\omega^2 + jX_3\omega + X_4}{-jl_1\omega^3 - l_2\omega^2 + jl_3\omega + l_4}\right\} \\ &= \frac{j\left\{l_1\omega^5 J - \omega^3 X_1 - \omega^3 l_3 J + \omega X_3\right\} + \left\{\omega^4 l_2 J - l_4\omega^2 J - \omega^2 X_2 + X_4\right\}}{-jl_1\omega^3 - l_2\omega^2 + jl_3\omega + l_4} \\ &= \frac{N_1(\mathrm{j}\omega)}{D_1(\mathrm{j}\omega)} \end{aligned} \quad (58)$$

where,

$$\begin{aligned} N_1(\mathrm{j}\omega) &= \mathrm{M}_1 + jN_1 \\ D_1(\mathrm{j}\omega) &= \mathrm{P}_1 + jQ_1 \end{aligned} \quad (59)$$

$$T_1(\mathrm{s}) + \mathrm{Js}^2\,|_{s=j\omega} = \left\{\frac{M_1 + jN_1}{P_1 + jQ_1}\right\} \quad (60)$$

where,

$$\begin{aligned} M_1 &= \omega^4 l_2 J - l_4\omega^2 J - \omega^2 X_2 + X_4 \\ N_1 &= l_1\omega^5 J - \omega^3 X_1 - \omega^3 l_3 J + \omega X_3 \\ P_1 &= l_4 - l_2\omega^2 \\ Q_1 &= \omega l_3 - \omega^3 l_1 \end{aligned} \quad (61)$$

$$D(s) = \frac{F_3(\mathrm{s})}{T_1(\mathrm{s}) + \mathrm{J}s^2} \quad (62)$$

$$D(\mathrm{j}\omega) = \frac{(\mathrm{A}_3\mathrm{P}_1 - B_3\mathrm{Q}_1) + \mathrm{j}(\mathrm{B}_3\mathrm{P}_1 + \mathrm{A}_3\mathrm{Q}_1)}{M_1 + jN_1} \quad (63)$$

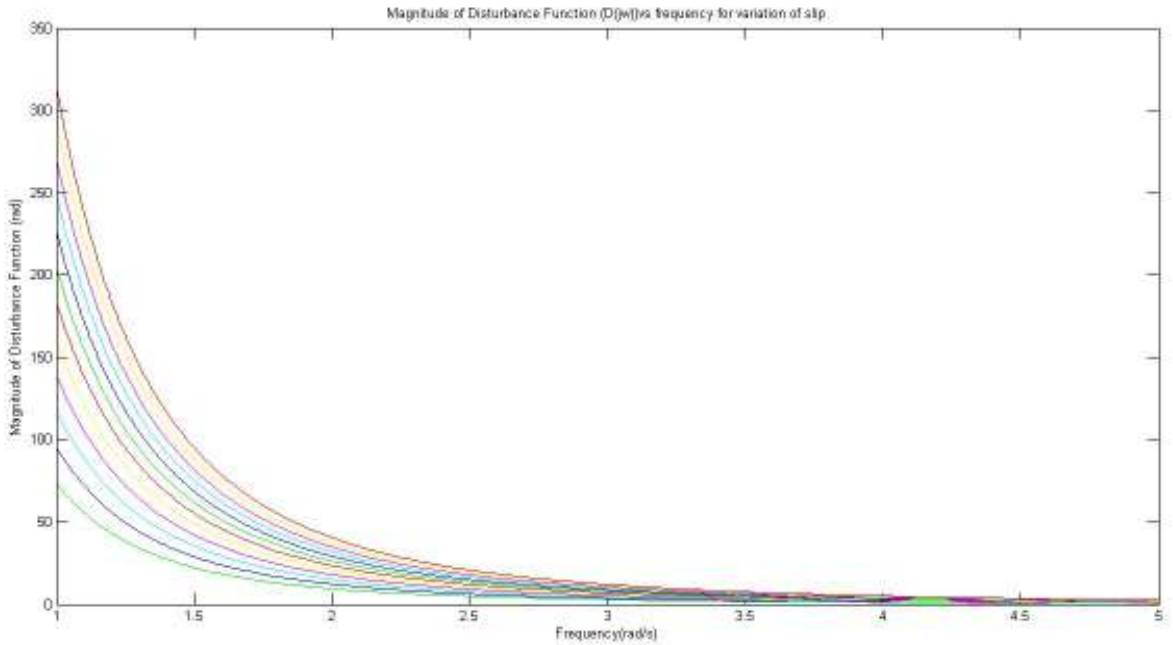

Fig. 4: Magnitude of the |D(jω)| plotted against ω

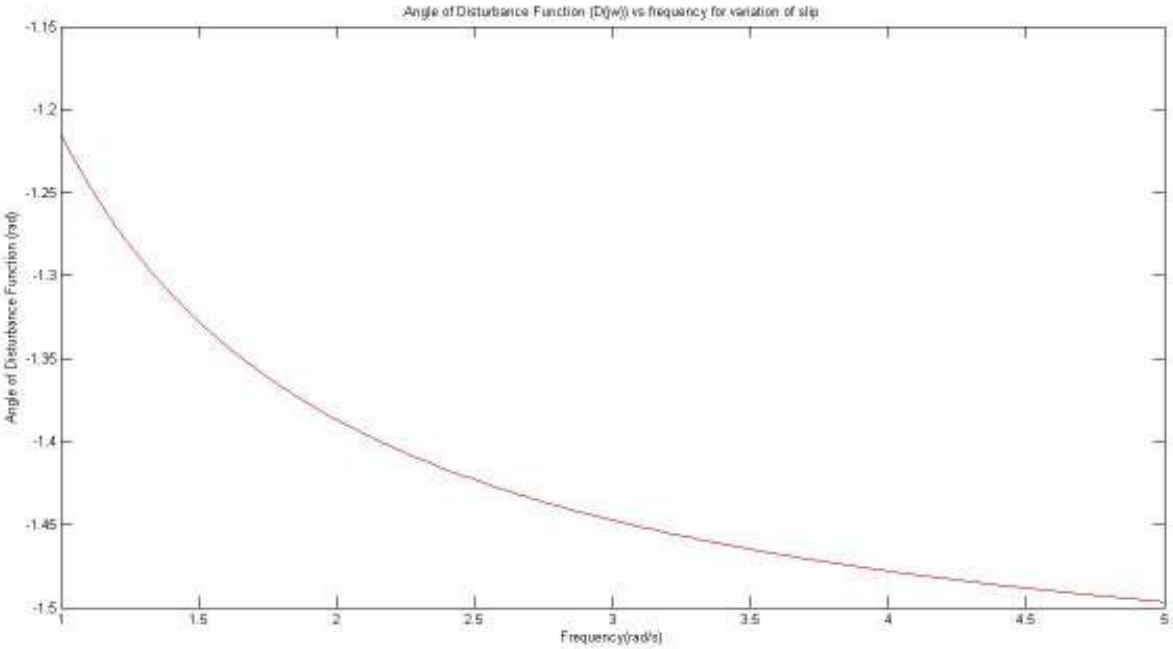

Fig. 5: Angle of the |D(jω)| plotted against ω

$$|\,\mathrm{D}(\mathrm{j}\omega)\,| = \frac{\sqrt{(\mathrm{A}_3\mathrm{P}_1 - B_3\,\mathrm{Q}_1)^2 + (\mathrm{B}_3\mathrm{P}_1 + \mathrm{A}_3\mathrm{Q}_1)^2}}{\sqrt{M_1^{\,2} + N_1^{\,2}}} \tag{64}$$

$$\angle D(\mathrm{j}\omega) = \tan^{-1}\left(\frac{\mathrm{B}_3\mathrm{P}_1 + \mathrm{A}_3\mathrm{Q}_1}{\mathrm{A}_3\mathrm{P}_1 - B_3\,\mathrm{Q}_1}\right) - \tan^{-1}\left(\frac{N_1}{M_1}\right) \tag{65}$$

The overall mathematical treatment basically interprets the role of induction motor action just before switching to synchronous motor action in a convenient mathematical from in the complex frequency domain. The motivation to formulate this problem in **s** domain (complex frequency domain) is not intentional rather it is a natural tendency because this paper may be treated as an extension of Chattopadhyay *et al*. (2011) in that paper the whole intention of the author were to investigate the steady state stability aspects using small perturbation model and that is why the formulation was

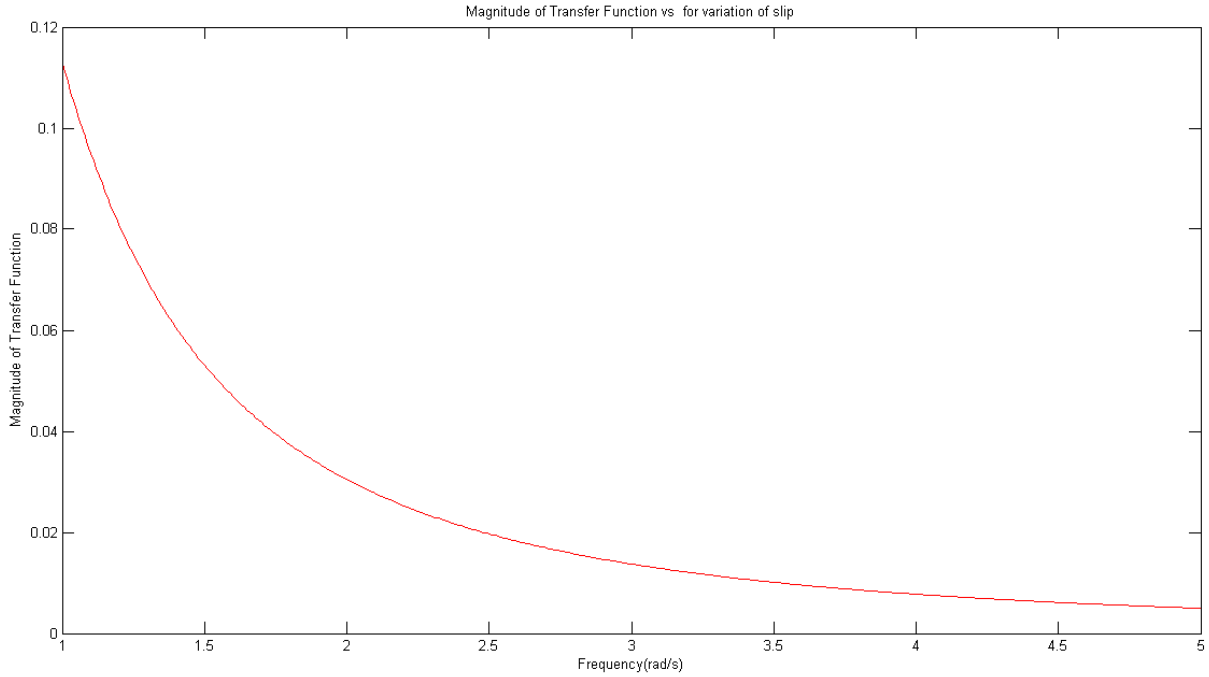

Fig. 6: Magnitude of the transfer function plotted against ω

finalized in's' domain. As an extension to such motivation it reveals that investigations can be made on the same machine just before switching to synchronous motor action (running as an induction motor). The overall model in complex frequency domain in the form of small perturbation model taking the role of induction motor into account does not lead to stability assessment model, however the nature if the function D(s) can be investigated in the marginal condition after substituting s = jω. After such mathematical substitution the function D(jω) involves magnitude and phase angle plot against 'ω' and such behavior are similar to analog filter characteristics. Hence the role of induction motor action for a physical synchronous motor may be looked upon as an analog filter behavior in the pure frequency domain in the concerned mathematical model. Those magnitude and phase angle plots of D(jω) are shown in Fig. 4 and 5. As the role of D(s) can be looked upon as a disturbance function in relation to the model given by equation D(S) = $\frac{F_3(S)}{T_1(S)+JS^2}$. In the equation, one part T(s) = $\frac{1}{T_1(S)+JS^2}$ can be treated as transfer function of the pure synchronous motor behavior of the same physical synchronous m/c similar to D(jω) formulation, T(s) can be converted to T(jω) after substitution of s = jω in the said function. The magnitude and phase angle plot of T(jω) against 'ω' are shown in Fig. 5 and 6. Even though the plots in Fig. 3 to 6 are based on the equation they need some physical explanation and the corresponding interpretation are presented in the next section.

RESULTS AND DISCUSSION

Magnitude of the |D(jω)| (Fig. 4) plotted against ω shows inverse functions and also a family of plot is obtained by varying slip. It is already known that:

$$D(\mathrm{j}\omega) = \frac{F_3(\mathrm{j}\omega)}{T_1(\mathrm{j}\omega) + \mathrm{J}(\mathrm{j}\omega)^2}$$

It may be recalled that during the period of induction machine action $[T_1(S) + JS^2]\,\Delta\beta(S) + F_3(S) = \Delta T_L(S)$, where each function has been expressed in the equations. Hence $F_3(s)$ can be treated as an equivalent to additional transformed load torque. This additional function has appearance due to the role of the induction motor when synchronous motor has started as an induction machine with the help of damper windings we know that roughly induction motor torque is an increasing function of slip in the steady state zone. The transformations from time domain has been obtained using Laplace operator and ultimately the formulation is obtained in the complex frequency domain (in terms of kernel s). Hence the physical transformation from synchronous machine to induction machine during the starting period should not be confused with the mathematical transformations from time domain to Laplace domain and hence the role of slip remains same in Laplace domain as in time domain. The function $[T_1(S) + JS^2]$ in Laplace domain appears due to the induced dynamics of the physical synchronous machine when it is exactly running as synchronous machine. Therefore the parameter slip

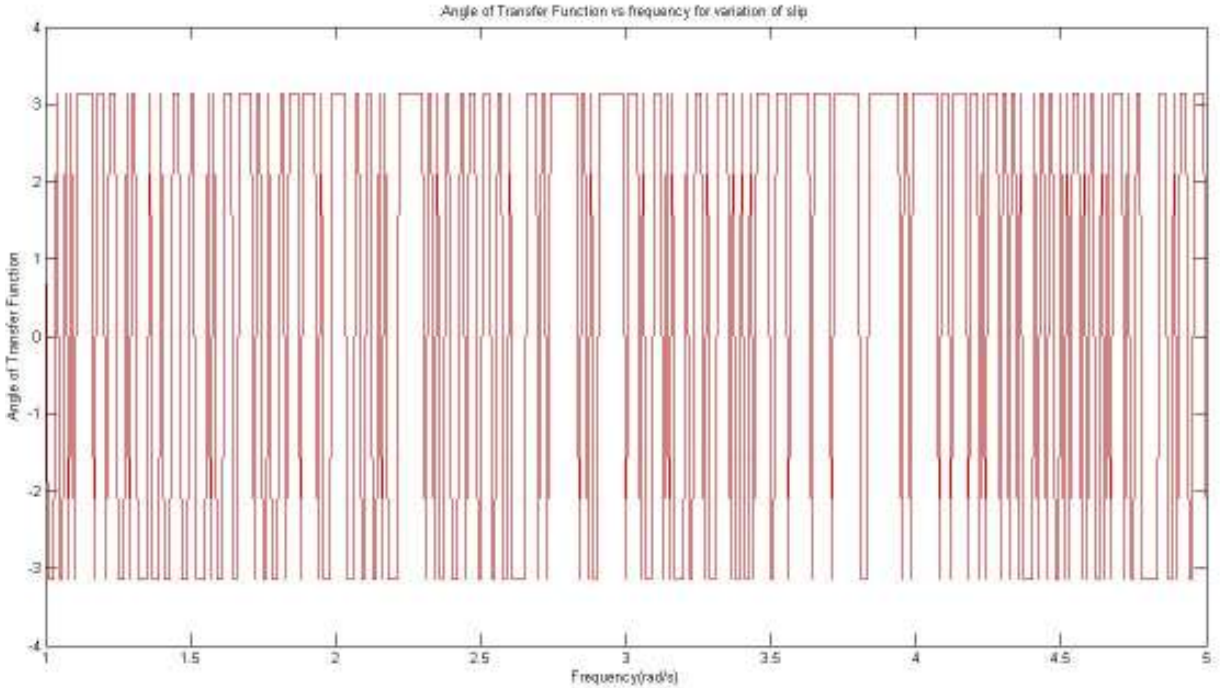

Fig. 7: Angle of the transfer function plotted against ω

from the view point of engineering conception should not affect this function and furthermore it is well known that slip is the indication of an asynchronous machine.

Explanation of the magnitude plot of D(jω) vs ω at a particular value of slip: Again we shall recall the function $\frac{1}{T_1(S)+JS^2}$, it has been observed that $[T_1(S) + JS2$ at s = jω, has a numerator polynomial containing highest power ω^3 and denominator ω^5 hence such functions should show dominance near zero frequency. Now let us separately concentrate on the function $F_3(s)$ which has a real part containing highest power ω^2 and negative imaginary parts containing highest power ω^3. Hence D(jω) which is product of $F_3(j\omega)$ and $\frac{1}{T_1(S)+JS^2}$, -- must be dictated by profile of $\frac{1}{T_1(S)+JS^2}$, at s=jω , when ω is varied. That is why in the plot of |D(jω)| vs ω shows inverse function at a particular value of sip with high dominance around zero frequency.

Figure 5 represents the plot of ∟ D(jω) against ω based on Eq. (65). It may be reminded that in Eq. (65) the angle of $F_3(s)$ at s = jω can be estimated very roughly as $tan^{-1}\left[\frac{\frac{1}{\omega^3}-\frac{1}{\omega}}{-\frac{1}{\omega^2}}\right]$ such rough expression will help the designer to predict the nature of the variation. The above said variation has a decaying nature with respect to ω. however the other part of the D(jω) function which is $T(j\omega) = \frac{1}{T_1(S)+JS^2}$ at s = jω has an oscillatory behavior of its phase angle with respect to ω. This oscillatory behavior of ∟ T(jω) vs ω can be easily interpreted because this function can be treated roughly as $\tan^{-1}(\omega)$ and that is why it is bounded between some specific values of angle (3.14). This behavior is plotted in Fig. 7. The plot of ∟ D (jω) vs ω involves the behavior of ∟ T (jω) vs ω but the dominance of ∟ F_3 (jω) is more, that is why the overall plot of ∟ D(jω) vs ω shows a dragging nature and it is plotted in Fig. 7. With reference to equation $\Delta\beta(j\omega) = T(j\omega)\ \Delta T_L - D(j\omega)$ at this stage only the interpretation of the plot of T(jω) remains as pending because the other 3 plots (Fig. 4 to 7) have been interpreted. The pending interpretation for Fig. 6 is as follows:

$$T(s) = \frac{1}{T_1(S)+JS^2},$$

at s = jω , hence $T(j\omega) = \frac{1}{T_1(j\omega)-J\omega^2}$,

$\frac{1}{T_1(j\omega)-J\omega^2}$ has a denominator polynomial in ω, having highest power 5. Hence at the high frequency region, |T(jω)| decreases very fast. This plot is shown in Fig. 6.

CONCLUSION

- Role of Induction motor in Laplace domain appears as an equivalent "system" consisting of multi-frequencies.
- Filtering of the equivalent "NOISE" may not be needed due to natural attenuation.
- To avoid or minimize George's phenomenon during the transition zone, inclusion of external

resistance in the field circuit basically leads to a complicated mathematical formulation, but clubbing this resistance along with the original field winding resistance develops the problem formulation in a more straight forward manner.

- With reference to Fig. 3, the time-frequency contour of the function (in s-domain), D(s) can be developed using STOCKWELL-Transform(S-Transform) and such contour will be able to provide more design information to the designer.

List of symbols:

i_d = Current in the D coil in p.u.
i_q = Current in the Q coil in p.u.
i_f = Current in the F coil in p.u.
i_{kd} = Current in the d axis damper coil (KD) in p.u.
i_{kq} = Current in the q axis damper coil (KQ) in p.u.
L_d = Self-inductance of D coil in p.u.
L_q = Self-inductance of Q coil in p.u.
L_{md} = Mutual inductance along d axis in p.u.
L_{mq} = Mutual inductance along q axis in p.u.
L_{ff} = Self-inductance of F (field) coil in p.u
R_f = Resistance of the F (field) coil in p.u.
L_{kd} = Self-inductance of the KD coil in p.u.
R_{kd} = Resistance of the KD coil in p.u
L_{kq} = Self-inductance of the KQ coil in p.u.
R_{kq} = Resistance of the KQ coil in p.u
β = Angle between the field (rotor) m.m.f. axis and armature (stator) m.m.f. axis

The machine data are given as (Xianhao *et al*., 2006):

J = 8 p.u.
L_d = 1.17 p.u.
L_{md} = 1.03 p.u.
L_q = 0.75 p.u.
L_{mq} = 0.61 p.u.
L_{kkd} = 1.122 p.u.
L_{kkq} = 0.725 p.u.
L_{ff} = 1.297 p.u.
R_{kd} = 0.03 p.u.
R_{kq} = 0.039 p.u.
R_f = 0.0015 p.u.

- When machine is at load:

i_s = 1 p.u.
i_{f0} = 0.97 p.u.
i_{kd0} = 0 p.u.
i_{kq0} = 0 p.u.
β_0 = 10^0

- When machine is at no load:

i_s = 0.1 p.u.
i_{f0} = 0.9 p.u.
i_{kd0} = 0 p.u.
i_{kq0} = 0 p.u.
β_0 = 0^0

REFERENCES

Al-Ohaly, A.A., R.M. Hamouda and M.A. Badr, 1997. Torsional oscillation associated with starting of three phase synchronous motors from a single phase supply. IEEE Trans. Energ. Conver., 12(1): 10-16.

Chattopadhyay, A.B., T. Sunil and C. Ruchira, 2011. Analysis of steady state stability of a Csi fed synchronous motor drive system with damper windings included. Trends Appl. Sci. Res., 6(9): 992-1005.

Das, J.C. and J. Casey, 1999. Characteristics and analysis of starting of large synchronous motors. Proceeding of the Industrial and amp; IEEE Conference on Commercial Power Systems Technical Conference, Sparks, NV.

Gordon, R.S., S.B. Dewan and W.A. Wilson James, 1974. Synchronous motor drive with current-source inverter. IEEE T. Ind. Appl., IA-10(3): 412-416.

Isfahani, A.H. and S. Vaez-Zadeh, 2011. Effects of magnetizing inductance on start-up and synchronization of line-start permanent-magnet synchronous motors. IEEE T. Magnet., 47(4): 823-829.

Knight, A.M. and C.I. McClay, 2000. The design of high-efficiency line-start motors. Proceeding of the 34th IAS Annual Meeting, Industry Applications Conference, Conference Record of the 1999 IEEE, 1: 516-522.

Marx, D., S. Pierfederici and B. Davat, 2008. Nonlinear control of an inverter motor drive system with input filter-large signal analysis of the DC-link voltage stability. Proceeding of the IEEE Power Electronics Specialists Conference, PESC, Rhodes, U.S.A, pp: 498-503.

Najafi, S. and N.C. Kar, 2007. Effect of short-circuit voltage profile on the transient performance of saturated permanent magnet synchronous motors. Proceeding of the IEEE Power Engineering Society General Meeting, Tampa, FL, pp: 1-6.

Sergelen, B., 2007. Mathematical model of salient pole synchronous motors supplied by a frequency converter. Proceeding of the International Forum on Strategic Technology, IFOST 2007, Ulaanbaatar, pp: 390-393.

Wang, X. and N. Ren, 2003. Simulation of asynchronous starting process of synchronous motors based on matlab/simulink. Proceeding of the 6th International Conference on Electrical Machines and Systems, ICEMS, Beijing, China, 2: 684-687.

Weifu, L., L.Yingli and Z.Haisen, 2012. Influences of rotor bar design on the starting performance of line-start permanent magnet synchronous motor. Proceeding of the 6th International Conference on Electromagnetic Field Problems and Applications (ICEF), Dalian, Liaoning, pp: 1-4.

Xianhao, M., S. Ding and W. Li, 2006. Calculation and analysis of magnetic fields and temperature fields for salient pole synchronous motors in the process of starting. Proceeding of the International Conference on Power System Technology, Chongqing, pp: 1-6.